Protein Folding

DOI: 10.1002/anie.201008040

Characteristics of Human Lysozyme and Its Disease-Related Mutants in their Unfolded States**

*Friederike Sziegat, Julia Wirmer-Bartoschek, and Harald Schwalbe**

Unfolded and partially folded states of proteins play a crucial role in the formation of fibril aggregates in human neurodegenerative diseases.[1–4] Some disease-associated proteins adopt well-folded structures in their native states while others belong to the class of intrinsically unstructured proteins.[5,6] The conversion of a soluble form of a protein to the aggregated state is typically related to the transient formation of unfolded or partially folded states for both classes of proteins. In many protein-folding diseases, single-point mutations, often inherited, are linked to specific disease forms but the structural code for the onset of the disease is still unclear.[7,8] Single-point mutations do not significantly change the structure of the native state.[9–12] Their impact on the structural and dynamic characteristics of the unfolded or intrinsically unstructured state ensemble remains a key unsolved question in structural biology.[13]

One of the approximately 20 amyloid diseases known to date is associated with the deposition of amyloid plaques from single-point mutants (I56T, F57I, I59T, W64R, and D67H) of human lysozyme (hLys)[14] in various organs. Given the remarkable high stability of this protein family, the discovery of protein-folding diseases associated with hLys came as a surprise.

Initial studies revealed that the native-state structures of wildtype (wt) and amyloidogenic mutants of hLys are highly similar.[9] Characterization of the thermal unfolding at pH 1.2 using CD spectroscopy, differential scanning calorimetry (DSC), and NMR spectroscopy showed that unfolding proceeds through loss of tertiary structure, resulting in a premolten globule state, which unfolds further as the temperature increases.[15] The β domain and the adjacent helix 3 (residues 90–100) unfold first. The same region is destabilized in the mutants as shown by hydrogen exchange,[16,17] leading to lower thermal stability.[9] This decrease in stability suggests that the relative stabilities of the folded and unfolded states are important in the process of amyloid formation. In fact, amyloid fibrils are formed fastest when the protein is incubated at very low pH (1.2) and at temperatures near the midpoint of thermal unfolding,[15] thus at a temperature at which folded as well as molten globule and premolten globule states, referred to here as unfolded states, are populated. For a better understanding of the mechanism leading to the formation of amyloid diseases, both folded and unfolded states therefore need to be characterized.

In contrast to the folded state of hLys, little is known about the residual structure and dynamics of its nonnative unfolded state. Heteronuclear NMR spectroscopy permits the characterization of not only the structure but also the dynamics of unfolded nonnative protein ensembles at atomic resolution. To highlight the remarkable influence of the mutants on the structure and dynamics in unfolded hLys, we first compare the unfolded states of the hen egg white lysozyme (hewl)and hLys to highlight the intrinsic higher aggregation propensity of hLys relative to that of hewl, and then discuss how two amyloidogenic mutants modulate the structure and dynamics of the premolten globule state of hLys.

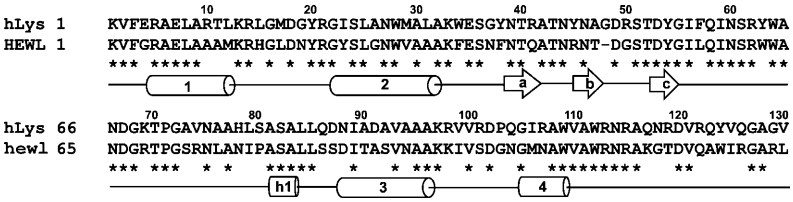

Scheme 1. Sequence alignment of the human (hLys) and hen egg-white (hewl) lysozyme[18] with residue numbers of hLys (identical amino acids are marked with asterisks). Cylinders 1, 2, 3, and 4 indicate α helices in the native states, h1 indicates the 3_{10} helix, and the arrows a, b, and c indicate β sheets.

The cysteine-to-alanine mutants of the proteins were investigated in the absence of chemical denaturants. Previous data for hewl showed that such an approach unravels the conformational propensities of the polypeptide chain without bias imposed by disulfide bridges and is closest to the conditions for stabilization of premolten globule states. This reduced state cannot fold; however, previous studies revealed that amyloid fibrils can be formed from reduced as well as from oxidized lysozymes.[19]

High sequence homology (≈70%) and identity (≈60%) are shared by hLys and hewl (Scheme 1). The native-state structures of hLys and hewl are very similar with a backbone

[*] F. Sziegat, Dr. J. Wirmer-Bartoschek, Prof. Dr. H. Schwalbe
Institute for Organic Chemistry and
Chemical Biology Center of Biomolecular Magnetic Resonance
J. W. Goethe University Frankfurt
Max-von-Laue-Strasse 7, 60439 Frankfurt (Germany)
Fax: (+49) 69-7982-9515
E-mail: schwalbe@nmr.uni-frankfurt.de
Homepage: http://schwalbe.org.chemie.uni-frankfurt.de

[**] This work was supported by the state of Hesse within the Center of Biomolecular Magnetic Resonance (BMRZ) and the DFG (Schw10/1). H.S. is a member of the DFG-funded Cluster of Excellence "macromolecular complexes".

Supporting information for this article is available on the WWW under http://dx.doi.org/10.1002/anie.201008040.

root mean square deviation (RMSD) of only 0.74 Å.[20] Their structure possesses two domains: an α domain (residues 1–38 and 86–130) with four α helices, and a β domain (residues 39–85) with a triple-stranded β sheet and a 3_{10} helix. Scheme 1 shows the amino acid sequences of both proteins; the two amyloidogenic mutation sites I56T and D67H are highlighted. Differences in the amino acid sequence are predominantly found between residues 70–80, 85–92, and 98–110, located at the interface between the α and the β domains.

Figure 1a compares H_N chemical shift deviations of the unfolded proteins from reference data obtained from random-coil peptides[21] and Figure 1b shows secondary-structure propensities (SSPs)[22] obtained from C_α and C_β chemical shifts. Both proteins show regions with significant chemical shift deviations. The deviations indicate transient formation of α-helical structures and cluster around residues 23–36, 53–65, 79–94, and 107–116 in hLys and residues 7–14, 23–38, 57–68, 107–116, and 121–125 in hewl.

In Figure 1c–f, spectral densities $J(\omega)$, $\{^1H\}$-^{15}N heteronuclear Overhauser effects (hetNOEs), and ^{15}N longitudinal R_1 and transverse R_2 relaxation rates of the two proteins are shown. For hLys, mainly positive hetNOE values are observed, whereas hetNOE values are negative for hewl with few exceptions. Positive hetNOE data in hLys are observed particularly for residues 11–24, 33–69, 81–91, and 108–116, while negative values are found at the termini and for residues 72–80 and 97–107. We conclude that the structural deviation towards the helical nonrandom structure is thus accompanied by restricted mobility of the polypeptide chain. To further evaluate the changes in the dynamics of the polypeptide chain, we analyzed the relaxation rates using the spectral density approach. In the analysis of the spectral density values (Figure 1c),[26,27] the dynamics of a given NH vector are reduced to a single motion where the spectral density at frequency ω is described by a Lorentzian line as $J(\omega) = J(0)/(1+6.25(\omega J(0))^2$. Residues with $J(\omega_N)/J(0)$ correlation near the ascending part of the Lorentzian curve are dominated by fast internal motions, while residues near the descending part (with $J(0) = 0.4\tau_c$) are rigid and dominated by overall tumbling. For residues exhibiting chemical exchange, $J(0)$ is increased by the exchange contribution, resulting in $J(0)$ values shifted to the right. For both proteins, the polypeptide chains undergo fast dynamics dominated by internal motions (for comparison, relaxation data are also provided for hewl under native conditions[24]). The variation observed for individual residues is greater for hLys than for hewl; this reflects the range from very flexible residues to residues that have contributions from both fast and slow motions. Particular high $J(0)$ values indicating higher rigidity are found for residues 33, 34, 56, 60–64, 89, 98, 111, and 112 in hLys.

In Figure 1e,f, the R_1 and R_2 relaxation rates of hLys and hewl are compared. For both proteins, the relaxation rates show smooth profiles, and variations along the sequence have a similar shape for R_1 and R_2. The R_1 data range up to around 1.8 s^{-1} while the R_2 rates range up to 6 s^{-1} for hLys and 5 s^{-1}

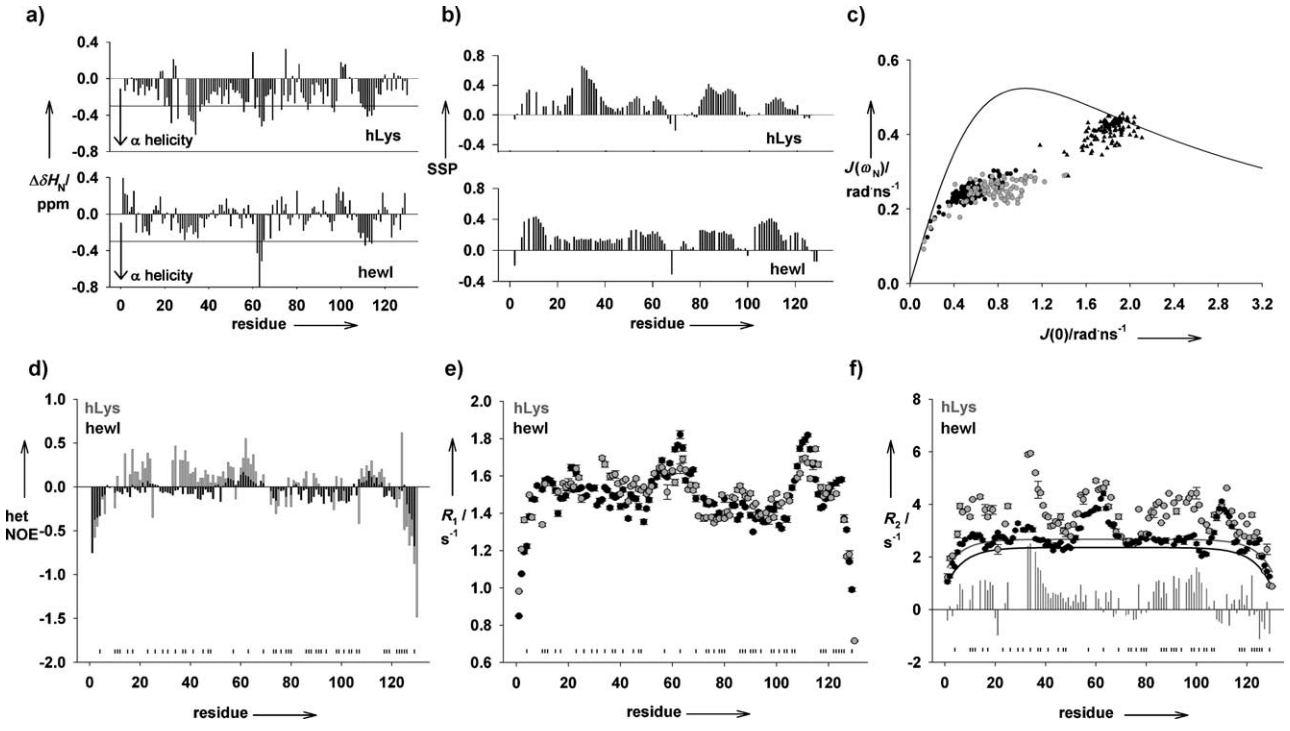

Figure 1. a) Chemical shift deviations from random-coil values of hLys and hewl ($\Delta\delta = \delta^{exp} - \delta^{rc}$). The gray lines indicate cut-offs for chemical shift indexing for the α helices at −0.3 ppm.[23] b) Secondary-structure propensities (SSPs)[22] of hLys and hewl. c) Spectral densities of hewl (black), hLys (gray), and native hewl (black triangle).[24] d–f) Comparison of heteronuclear ^1H-^{15}N hetNOEs, and R_1 and R_2 relaxation rates of hLys (gray) and hewl (black). The gray bars in (f) indicate the difference in the R_2 rates of hLys and hewl. Small vertical marks in (d–f) indicate differing amino acids in the sequences of hlys and hewl. All experiments were carried out at 600 MHz with a protein concentration of 300 μM at pH 2 (water, 10% D_2O), 293 K.

for hewl; variations along the sequence are thus more pronounced for the R_2 data.

The observed overall R_2 relaxation rates for hLys are higher than those for hewl. In theory, such behavior is either due to the increased rigidity or the presence of a conformational exchange process with rate constants $k_{ex} \approx 2/\zeta$, where ζ is the time between two Carr–Purcell–Meiboom–Gill (CPMG) pulses during relaxation measurements[25] (here $\zeta = 900$ μs). There are multiple methods to support the presence of chemical exchange processes in unfolded states of proteins including relaxation dispersion measurements and analysis of $J(\omega_N)/J(0)$ and the shape of the measured R_2 rates: R^{ex} is proportional to $\Delta\omega^2$ ($\Delta\omega$ = chemical shift difference between exchanging conformers[25]); $\Delta\omega$ is not continuous over the sequence but scatters, and as a consequence R_2 relaxation rates in the presence of exchange are also scattered (e.g. as observed in SH3 of drkN for residues 25–28[28,29]). Based on the $J(\omega_N)/J(0)$ analysis and the absence of significant scatter in the relaxation rates as well as the relaxation dispersion and R_{1rho} measurements (R_{1rho} = spin–lattice relaxation rates in the rotating frame, Figures S1 and S2 in the Supporting Information), we can exclude that the elevated level of relaxation rates in hLys at a concentration of 300 μM stems from chemical exchange processes.

Hewl contains six hydrophobic clusters around 1) A9, 2) W28, 3) W62/W63, 4) L83, 5) W108/W111, and 6) W123.[30] Similarly, six clusters are found in hLys around 1) L12, 2) W28/W34, 3) Y63/W64, 4) V93, 5) W109/W112, and 6) Y124. The relative sizes of the clusters differ for the two proteins (difference plot in Figure 1 f) while the overall cluster architecture remains the same. The cluster with the highest relaxation rates in hLys is cluster 2 with W28 and W34. Cluster 2 is not dominant in hewl, which contains a phenylalanine at position 34 rather than a tryptophan. Clusters 1, 3, 4, and 5 have approximately the same amplitudes (with R_2 rates ranging from 1.8 to 3.2 s^{-1}) while cluster 6 is very small in hLys. The most striking difference is found in cluster 4 (residues 78–105). This cluster is only marginally present in hewl, while it is very prominent in hLys although it does not contain any aromatic residue. Residues in this region of the polypeptide chain are at the interface between the two domains and form a 3_{10} helix (residues 81–85) and an α helix (helix 3, residue 90–100) in the native proteins (Figure 2).

In this region of the polypeptide chain the two proteins differ most in their primary sequence (Scheme 1). While positively charged and neutral residues are found in cluster 4 of hewl at acidic pH, the region is predominantly neutral in hLys; this explains the observed differences by the absence of charge repulsion and a potential increase in the hydrophobic interactions. It is indeed the region of the β domain and the adjacent helix 3 which is the first region involved in to the formation of amyloid fibrils.[17]

Formation of amyloid fibrils occurs neither from the folded conformation nor from a completely unstructured state but from some partially structured state capable of aggregating.[15,31–33] We therefore conclude that the degree of residual structure and restriction of dynamics in hLys relative to those of the homologous hewl correlate with the increased tendency of hLys to form amyloid fibrils. This conclusion is

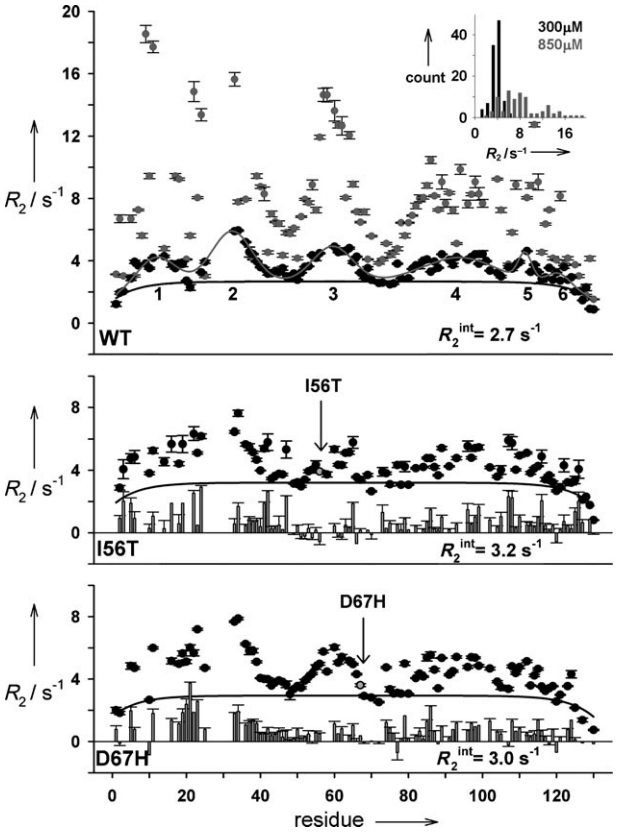

Figure 2. R_2 relaxation rates of hLys (top; black: protein concentration 300 μM, gray: 850 μM), hLysI56T (middle), and hLysD67H (bottom, conditions for all: 600 MHz, 300 μM, pH 2, 293 K). Black line: R_2^{rc} baseline, gray line: fit for the wildtype, and gray bars: difference in mutant R_2 and wildtype R_2. Inset in the top panel: histogram of R_2 rates recorded for protein concentrations of 850 and 300 μM.

further supported by data of hLys recorded at different concentrations (Figure 2 top and Figure S2–S5 in the Supporting Information): increased R_2 relaxation rates and in particular scatter in the regions of clusters 1, 2, 4, 5, and 6 are observed at higher protein concentration, while the R_1, hetNOE, and R_{1rho} values remain qualitatively the same regardless of concentration. The highest R_2 rates range up to 18.5 s^{-1} for A9 and 17.7 s^{-1} for T11. The scatter and height of the rates as well as the big difference between the R_2 and R_{1rho} data are indicative of exchange. Both the increase of rigidity reflected by the overall higher relaxation rates and the presence of exchange indicate most likely the transient formation of oligomers in the sample at higher concentration.

We then investigated two amyloidogenic mutants of hLys at low concentration. Figure 2 shows R_2 relaxation rates of the I56T and the D67H mutant relative to those of the wildtype sequence. The relaxation rates are significantly higher in the amyloid-linked forms than in the wt sequence at low concentration including elevated R_2^{rc} baselines ($R_2^{rc} = R_2$ rate expected for random-coil, black line) and additional deviations from the baseline. This is in contrast to previous data on hewl-S^{Me}, where single-point mutations led to significantly reduced relaxation rates.[30] The highest relaxation rates are observed for the mutant D67H with 7.7 and 7.9 s^{-1} for K33

and W34 in cluster 2. In contrast to the wildtype sequence, significant scatter is observed. While the overall cluster structure is retained between hewl and hLys, the amyloidogenic single-point mutations disrupt the cluster architecture in the premolten globule state of hLys. Clusters 1 and 2 merge in both mutants to a broad cluster with significant scatter. Cluster 3 is retained and slightly elevated in the D67H mutant while a slight reduction of the R_2 rates around the mutation site is observed for I56T. While clusters 4, 5, and 6 are clearly separated in the wt sequence, the clustered structure in this area vanishes and we observe scattering with values up to 5.9 s^{-1}. The spectral density analysis of the mutants reveals higher $J(0)$ values while $J(\omega)$ remains rather constant (Figure S6 in the Supporting Information). Particularly large shifts are observed for I23, K33, and W34 in D67H, and K33 and W34 in I56T. Both the significant scattering and increased $J(0)$ value are indicative of chemical exchange processes in the mutants. The mutants thus show reduced flexibility and exchange even at low concentration which might be due to the formation of oligomeric aggregates within the sample.

To test this hypothesis, translational diffusion measurements[34] were performed (Table 1). The hydrodynamic radius (R_h) of hLys at a concentration of 300 μM is similar to the value of 26.9 Å previously determined for hewl-S^{Me}.[30] Aggregates of hLys are formed at higher concentrations as shown by an increase of 13% for R_h at a concentration of 850 μM. The mutants have larger hydrodynamic radii even at low concentration and these increase further as the concentration is increased. The data suggest that the mutations shift the onset of aggregation towards lower concentrations, while the concentration-dependent increase is similar (around 10%) for the three proteins.

Table 1: Hydrodynamic radii (R_h) of hLys and mutants obtained from translational diffusion measurements[34] (600 MHz in D_2O at pH 2, 293 K).

	$R_{h\,300\mu M}$ [Å]	$R_{h\,850\mu M}$ [Å]	R_h incr. [%]
hLys	26.7 ± 0.4	30.3 ± 0.2	13.5
D67H	30.3 ± 0.2	35.2 ± 0.5	16.2
I56T	31.9 ± 0.4	33.5 ± 0.3	10.5

We have examined the premolten globule unfolded states of the reduced states of hLys and two mutants using ^{15}N relaxation rates and chemical shift deviations. In contrast to the sequence- and structure-related α lactalbumin family, where cluster characteristics are altered,[35] the overall structural characteristics of hLys and hewl are remarkably similar: in both proteins six clusters around hydrophobic residues can be found. In detail, however, the wildtype sequence of hLys reveals greater chemical shift deviations, higher heteronuclear relaxation rates, and a larger spread in these rates. This observation is linked to a reduction of flexibility as evidenced by $J(\omega_N)/J(0)$ analysis (Figure 1b). In our previous work on hewl, we showed that nonconservative single-point mutations from W to G, located in hydrophobic clusters of the protein, disrupt the long-range order found in the nonnative wt protein.[30] The effects of disease-related mutations in hLys are different: partial disruption of the cluster structure, higher relaxation rates, and greater scatter of the rates, indicative of chemical exchange, are observed in the disease-related mutants. These effects are also observed in the wt sequence at high concentration.

The structures in Figure 3 display changes in the conformational dynamics mapped onto the native structure of hLys. Residues that are in the core of the native protein have lower flexibility (colored in white–red) in their unfolded state than those on the outside of the protein (colored in blue) with exception of the region around W62/Y63 which is exceptionally rigid in the unfolded state. The amyloidogenic mutations induce changes in the relaxation rates and increase rigidity. These changes cannot be explained by interactions present in the native structure, because relaxation rates are influenced in regions of the protein that do not interact with the mutation site. These results point towards nonnative interactions in the premolten globule state of the protein. They are also not explained by using a random-coil model without any interactions between parts of the protein that are distant in the sequence. The formation of transient oligomers may be a suitable explanation for this observation, taking into account the observed chemical exchange.

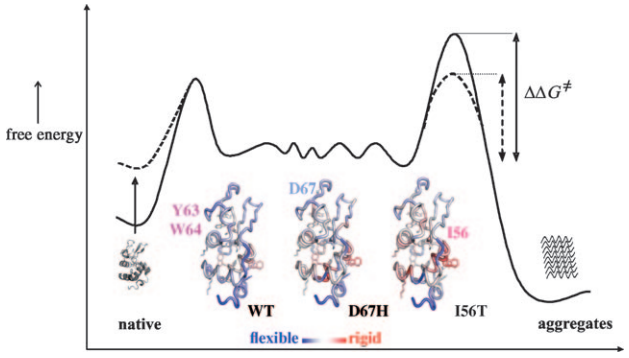

Figure 3. Proposed free-energy landscape for the unfolding and aggregation of hLys. The dashed lines indicate the energy levels for hLys while the solid lines are for hewl. The R_2 rates of the reduced proteins are mapped onto the structures of hLys (2zij.pdb[36]) with low R_2 rates (blue, flexible regions), medium R_2 rates (white), and high R_2 relaxation rates (red, rigid regions).

Figure 3 shows the free-energy landscape of hLys for native states, unfolded nonnative states, and aggregated fibrils. As previously reported,[9] single-point mutations do not change the structure of the native state but lead to a destabilization that results in significantly reduced melting temperatures of the mutants and an increase in the free energy of the native state. We show here that single-point mutantions have a pronounced effect on the free-energy landscape of the unfolded nonnative state ensemble. From our analysis of hLys and two of its disease-related mutants, we conclude that the profile of the energy landscape connecting different members of the ensemble of premolten states is affected by single-point mutations. While the overall compactness and formation of long-range hydrophobic clusters characteristic of the family of lysozymes is maintained, the

dynamics of the conformational ensemble is markedly different in the disease-related single-point mutants. The mutations therefore change the relative populations within the unfolded nonnative state ensemble towards transient populations of states that are capable of aggregating. These states consequently have a lower activation energy $\Delta\Delta G^{\ddagger}$ for the transition from the unfolded premolten globule state towards the aggregated state. Our model, therefore, implies a very subtle and fragile balance between maintaining the functional native state of the protein and avoiding mutations which, by changing the energetics of the folding landscape, lead to aggregation.

Received: December 20, 2010
Revised: April 6, 2011
Published online: May 5, 2011

Keywords: amyloid diseases · lysozymes · NMR spectroscopy · protein folding · proteins

[1] M. B. Pepys, T. W. Rademacher, S. Amatayakul-Chantler, P. Williams, G. E. Noble, W. L. Hutchinson, P. N. Hawkins, S. R. Nelson, J. R. Gallimore, J. Herbert et al., *Proc. Natl. Acad. Sci. USA* **1994**, *91*, 5602.
[2] S. B. Prusiner, *Science* **1997**, *278*, 245.
[3] L. C. Serpell, M. Sunde, C. C. Blake, *Cell. Mol. Life Sci.* **1997**, *53*, 871.
[4] C. M. Dobson, *Nature* **2003**, *426*, 884.
[5] K. K. Turoverov, I. M. Kuznetsova, V. N. Uversky, *Prog. Biophys. Mol. Biol.* **2010**, *102*, 73.
[6] K. Sugase, H. J. Dyson, P. E. Wright, *Nature* **2007**, *447*, 1021.
[7] M. B. Pepys, P. N. Hawkins, D. R. Booth, D. M. Vigushin, G. A. Tennent, A. K. Soutar, N. Totty, O. Nguyen, C. C. Blake, C. J. Terry et al., *Nature* **1993**, *362*, 553.
[8] L. A. Morozova-Roche, J. Zurdo, A. Spencer, W. Noppe, V. Receveur, D. B. Archer, M. Joniau, C. M. Dobson, *J. Struct. Biol.* **2000**, *130*, 339.
[9] D. R. Booth, M. Sunde, V. Bellotti, C. V. Robinson, W. L. Hutchinson, P. E. Fraser, P. N. Hawkins, C. M. Dobson, S. E. Radford, C. C. Blake, M. B. Pepys, *Nature* **1997**, *385*, 787.
[10] S. Barghorn, Q. Zheng-Fischhofer, M. Ackmann, J. Biernat, M. von Bergen, E. M. Mandelkow, E. Mandelkow, *Biochemistry* **2000**, *39*, 11714.
[11] D. C. Jenkins, I. D. Sylvester, T. J. Pinheiro, *FEBS J.* **2008**, *275*, 1323.
[12] D. B. Trivella, L. Bleicher, C. Palmieri Lde, H. J. Wiggers, C. A. Montanari, J. W. Kelly, L. M. Lima, D. Foguel, I. Polikarpov, *J. Struct. Biol.* **2010**, *170*, 522.
[13] E. H. Koo, P. T. Lansbury, Jr., J. W. Kelly, *Proc. Natl. Acad. Sci. USA* **1999**, *96*, 9989.
[14] C. Rocken, S. Wilhelm, *J. Lab. Clin. Med.* **2005**, *146*, 244.
[15] A. Dhulesia, N. Cremades, J. R. Kumita, S. T. Hsu, M. F. Mossuto, M. Dumoulin, D. Nietlispach, M. Akke, X. Salvatella, C. M. Dobson, *J. Am. Chem. Soc.* **2010**, *132*, 15580.
[16] M. Dumoulin, D. Canet, A. M. Last, E. Pardon, D. B. Archer, S. Muyldermans, L. Wyns, A. Matagne, C. V. Robinson, C. Redfield, C. M. Dobson, *J. Mol. Biol.* **2005**, *346*, 773.
[17] D. Canet, A. M. Last, P. Tito, M. Sunde, A. Spencer, D. B. Archer, C. Redfield, C. V. Robinson, C. M. Dobson, *Nat. Struct. Biol.* **2002**, *9*, 308.
[18] M. A. Larkin, G. Blackshields, N. P. Brown, R. Chenna, P. A. McGettigan, H. McWilliam, F. Valentin, I. M. Wallace, A. Wilm, R. Lopez, J. D. Thompson, T. J. Gibson, D. G. Higgins, *Bioinformatics* **2007**, *23*, 2947.
[19] A. J. Trexler, M. R. Nilsson, *Curr. Protein Pept. Sci.* **2007**, *8*, 537.
[20] C. Redfield, C. M. Dobson, *Biochemistry* **1990**, *29*, 7201.
[21] S. Schwarzinger, G. J. Kroon, T. R. Foss, P. E. Wright, H. J. Dyson, *J. Biomol. NMR* **2000**, *18*, 43.
[22] J. A. Marsh, V. K. Singh, Z. Jia, J. D. Forman-Kay, *Protein Sci.* **2006**, *15*, 2795.
[23] D. S. Wishart, B. D. Sykes, F. M. Richards, *Biochemistry* **1992**, *31*, 1647.
[24] M. Buck, J. Boyd, C. Redfield, D. A. MacKenzie, D. J. Jeenes, D. B. Archer, C. M. Dobson, *Biochemistry* **1995**, *34*, 4041.
[25] M. Akke, N. J. Skelton, J. Kordel, A. G. Palmer 3rd, W. J. Chazin, *Biochemistry* **1993**, *32*, 9832.
[26] H. Křížová, L. Žídek, M. J. Stone, M. V. Novotny, V. Sklenář, *J. Biomol. NMR* **2004**, *28*, 369.
[27] J. F. Lefèvre, K. T. Dayie, J. W. Peng, G. Wagner, *Biochemistry* **1996**, *35*, 2674.
[28] N. A. Farrow, O. Zhang, J. D. Forman-Kay, L. E. Kay, *Biochemistry* **1997**, *36*, 2390.
[29] M. Tollinger, N. R. Skrynnikov, F. A. Mulder, J. D. Forman-Kay, L. E. Kay, *J. Am. Chem. Soc.* **2001**, *123*, 11341.
[30] J. Wirmer, C. Schlorb, J. Klein-Seetharaman, R. Hirano, T. Ueda, T. Imoto, H. Schwalbe, *Angew. Chem.* **2004**, *116*, 5904; *Angew. Chem. Int. Ed.* **2004**, *43*, 5780.
[31] K. A. Conway, J. D. Harper, P. T. Lansbury, Jr., *Biochemistry* **2000**, *39*, 2552.
[32] C. Gerum, R. Silvers, J. Wirmer-Bartoschek, H. Schwalbe, *Angew. Chem.* **2009**, *121*, 9616; *Angew. Chem. Int. Ed.* **2009**, *48*, 9452.
[33] V. Kallhoff, E. Peethumnongsin, H. Zheng, *Mol. Neurodegener.* **2007**, *2*, 6.
[34] D. K. Wilkins, S. B. Grimshaw, V. Receveur, C. M. Dobson, J. A. Jones, L. J. Smith, *Biochemistry* **1999**, *38*, 16424.
[35] J. Wirmer, H. Berk, R. Ugolini, C. Redfield, H. Schwalbe, *Protein Sci.* **2006**, *15*, 1397.
[36] P. J. Artymiuk, C. C. Blake, *J. Mol. Biol.* **1981**, *152*, 737.

